Structure of Lithium Hexamethyldisilazide (LiHMDS) in the Presence of Hexamethylphosphoramide (HMPA). Spectroscopic and Computational Studies of Monomers, Dimers, and Triple Ions

Floyd E. Romesberg, Max P. Bernstein, James H. Gilchrist, Aidan T. Harrison, David J. Fuller, and David B. Collum*

Contribution from the Department of Chemistry, Baker Laboratory, Cornell University, Ithaca, New York 14853-1301

Received August 24, 1992

Abstract: [6]Li and ^{15}N NMR spectroscopic studies of [6]Li and ^{15}N isotopically labeled lithium hexamethyldisilazide ([[6]Li]LiHMDS and [[6]Li,^{15}N]LiHMDS) confirm Kimura and Brown's earlier conclusions that LiHMDS exists as a monomer–cyclic dimer mixture in THF, a single cyclic oligomer of indeterminate structure in toluene, and a mixture of two or more cyclic oligomers in pentane.[42] ^{15}N zero-quantum NMR spectroscopy provides the distinction of the THF-solvated dimers from the higher oligomers but provides ambiguous results for the cyclic oligomer observed in toluene-*d*₈. Complex equilibria are observed in LiHMDS/HMPA/THF mixtures using one-dimensional [6]Li, ^{15}N, and ^{31}P NMR spectroscopy in conjunction with [6]Li–[15]N and [31]P–[6]Li heteronuclear multiple quantum correlation spectroscopic methods. Stepwise solvation of monomers, dimers, and triple ions [e.g., $R_2N-Li-NR_2^-//^+LiS_4$] are readily monitored. Excess (>2.0 equiv per Li) HMPA affords a disolvated monomer and a tetrasolvated triple ion as the limiting structures. Enthalpies calculated using semiempirical (MNDO) computational methods reveal trends that are in good qualitative agreement with experiment.

Introduction

Hexamethylphosphoramide (HMPA) dramatically enhances the rates of a variety of organolithium reactions.[1] Although there exists a consensus that HMPA influences reactivity by dissociation of aggregates into highly reactive monomers, ion pairs, or free ions, this notion remained largely unchallenged for several decades.[2] The situation changed dramatically in 1989 when the groups of Reich[3] and Snaith[4] reported the first examples of two-bond [31]P–[6]Li and [31]P–[7]Li coupling in HMPA solvates, providing a vehicle of unparalleled importance for studying lithium ion solvation. In a very short time, Reich and co-workers reported aggregation and solvation states of a wide range of inorganic and organic lithium salts solvated by HMPA that seemed to be congruent with existing models.[5,6] However, further investigations

revealed unexpected subtleties of organolithium solvation by HMPA. Lithium diisopropylamide, for example, undergoes serial solvation of the dimeric form, but no detectable deaggregation occurs.[7] Addition of HMPA to THF solutions containing a mixture of monomeric and dimeric lithium 2,2,6,6-tetramethylpiperidide (LiTMP) affords *eight* distinctly different LiTMP–HMPA solvates, including such oddities as triple ions and open dimers.[7] Despite the substantial solvation state changes and structural readjustments, HMPA has little influence on the overall aggregation state. Jackman and Chen discovered that addition of HMPA to lithium phenolates causes a striking *increase* in the aggregation state from predominantly dimer to predominantly tetramer.[8]

We describe herein [6]Li, ^{15}N, and ^{31}P NMR spectroscopic studies[9] of lithium hexamethyldisilazide ([[6]Li]LiHMDS and [[6]Li,^{15}N]LiHMDS) in hydrocarbons, THF, and THF/HMPA mixtures. [6]Li–[15]N and [31]P–[6]Li heteronuclear multiple quantum correlation (HMQC) spectroscopies[10] and ^{15}N zero-quantum NMR spectroscopy[11] play central roles. The structure assignments for LiHMDS in THF and hydrocarbons are in full agreement with those of Kimura and Brown reported in 1971.[12] The LiHMDS equilibria in THF/HMPA are similar to those gleaned from the studies of LiTMP/THF/HMPA mixtures.[7] Semiempirical (MNDO) calculations of enthalpies correlate well with the spectroscopically observed structures.[14]

Results

The techniques for studying lithium amide solution structures are well established.[7,9] Selected spectra illustrate the general

(1) Wardell, J. L. In *Comprehensive Organometallic Chemistry*; Wilkinson, G., Stone, F. G. A., Abels, F. W., Eds.; Pergamon: New York, 1982; Vol. 1, Chapter 2. *Ions and Ion Pairs in Organic Reactions*; Szwarc, M., Ed.; Wiley: New York, 1972; Vols. 1 and 2.

(2) Physicochemical studies of lithium ion solvation by HMPA: Vandyshev, V. N.; Korolev, V. P.; Krestov, G. A. *Thermochim. Acta* **1990**, *169*, 57. Goralski, P.; Taniewska-Osinska, S.; Le Goff, D.; Chabanel, M. *J. Chem. Soc., Faraday Trans.* **1990**, *86*, 3103. Birkeneder, F.; Pollmer, K. *Z. Anorg. Allg. Chem.* **1990**, *583*, 152. Rannou, J.; Legoff, D.; Chabanel, M. *J. Chem. Res., Synop.* **1989**, 324. Mishustin, A. I. *Zh. Fiz. Khim.* **1988**, *62*, 3201. Perelygin, I. S.; Beloborodova, N. N.; Gryaznov, S. I. *Zh. Strukt. Khim.* **1987**, *28*, 66. Castagnolo, M.; Petrella, G.; Inglese, A.; Sacco, A.; Della, M. *J. Chem. Soc., Faraday Trans. 1* **1983**, *79*, 2211. Pestunovich, V. A.; Kruglaya, O. A.; Vyazankin, N. S. *Izv. Akad. Nauk SSSR, Ser. Khim.* **1980**, 53. Gilkerson, W. R.; Jackson, M. D. *J. Am. Chem. Soc.* **1979**, *101*, 4096. Mishustin, A. I.; Podkovyrin, A. I.; Kessler, Yu. M. *Dokl. Akad. Nauk SSSR* **1979**, *245*, 1420. Narula, S. P.; Banait, J. S.; Jauhar, S. P. *Z. Phys. Chem.* **1977**, *108*, 259. Osipenko, N. G.; Petrov, E. S.; Ranneva, Yu. I.; Tsvetkov, E. N.; Shatenshtein, A. I. *Zh. Obshch. Khim.* **1977**, *47*, 2172.

(3) Reich, H. J.; Green, D. P. *J. Am. Chem. Soc.* **1989**, *111*, 8729.

(4) Barr, D.; Doyle, M. J.; Mulvey, R. E.; Raithby, P. R.; Reed, D.; Snaith, R.; Wright, D. S. *J. Chem. Soc., Chem. Commun.* **1989**, 318. Raithby, P. R.; Reed, D.; Snaith, R.; Wright, D. S. *Angew. Chem., Int. Ed. Engl.* **1991**, *30*, 1011.

(5) Reich, H. J.; Green, D. P.; Phillips, N. H. *J. Am. Chem. Soc.* **1989**, *111*, 3444. Reich, H. J.; Borst, J. P. *J. Am. Chem. Soc.* **1991**, *113*, 1835.

(6) Denmark, S. E.; Miller, P. C.; Wilson, S. R. *J. Am. Chem. Soc.* **1991**, *113*, 1468. See also, Croisat, D.; Seyden-Penne, J.; Strzalko, T.; Wartski, L.; Corset, J.; Froment, F. *J. Org. Chem.* **1992**, *57*, 6435.

(7) Romesberg, F. E.; Gilchrist, J. H.; Harrison, A. T.; Fuller, D. J.; Collum, D. B. *J. Am. Chem. Soc.* **1991**, *113*, 5751.

(8) Jackman, L. M.; Chen, X. *J. Am. Chem. Soc.* **1992**, *114*, 403.

(9) Leading references: Hall, P.; Gilchrist, J. H.; Harrison, A. T.; Fuller, D. J.; Collum, D. B. *J. Am. Chem. Soc.* **1991**, *113*, 9575.

(10) Gilchrist, J. H.; Harrison, A. T.; Fuller, D. J.; Collum, D. B. *Magn. Reson. Chem.* **1992**, *30*, 855.

(11) Gilchrist, J. H.; Collum, D. B. *J. Am. Chem. Soc.* **1991**, *113*, 794.

(12) Kimura, B. Y.; Brown, T. L. *J. Organomet. Chem.* **1971**, *26*, 57.

3476 J. Am. Chem. Soc., Vol. 115, No. 9, 1993

Romesberg et al.

Table I. NMR Spectroscopic Data of [6Li]LiHMDS and [6Li,15N]LiHMDS Solvates[a]

compd	equiv of HMPA[b]	6Li δ (m, J_{N-Li}, J_{P-Li})[c]	15N δ (m, J_{N-Li})	31P δ (m, J_{P-Li})
(LiHMDS)$_n$	0.0	1.71 (t, 4.1, -, dimer)	45.8 (quint, 4.5)	
		1.63 (t, 3.5, -, olig)	45.9 (quint, 3.5)	
1	0.0	-0.26 (d, 5.0, -)	41.2 (t, 5.0)	
2	0.0	0.84 (t, 5.0, -)	38.3 (quint, 3.4)	
3	0.3	-0.04 (t, 5.0, 3.7)	41.1 (t, 5.0)	26.6[e] (t, 3.7)
4	2.0	0.24 (d, 5.0, -[d])	43.6 (t, 5.0)	26.7 (s, -[d])
5	0.3	0.34 (q, 3.2, 5.0)	37.8 (quint, 3.2)	25.9 (s, -[d])
		0.74 (t, 3.4, -)		
6	1.0	0.46 (q, 3.1, 5.0)	37.2 (quint, 3.1)	25.8 (t, 5.0)
7	0.8	1.22[f] (t, 5.0, -)	43.7 (t, 5.0)	26.9 (t, 4.2)
		-0.69 (t, -, 4.2)		
8	1.5	1.22[f] (t, 5.0, -)	43.7 (t, 5.0)	26.8 (t, 3.3)
		-0.59 (q, -, 3.3)		
9	2.0	1.25[f] (t, 5.0, -)	43.6 (t, 5.0)	26.8 (t, 2.9)
		-0.54 (quint, -, 2.9)		

[a] Spectra were recorded at the following temperatures: 6Li and 15N, -115 °C; 31P, -120 °C. [LiHMDS] = 0.13 M in a 2:1 THF/pentane cosolvent. The data for the unsolvated LiHMDS oligomers were obtained on a 0.12 M solution in pentane. Coupling constants were measured after resolution enhancement: s = singlet, d = doublet, t = triplet, q = quartet, quint = quintet. Chemical shifts are recorded relative to external standards, as described in the Experimental Section. All J values reported in hertz. [b] Equivalents of HMPA in the NMR sample from which the tabulated data are derived. [c] Distinction of Li–N from Li–P was made by comparison of [6Li]LiHMDS and [6Li,15N]LiHMDS. - means no data. [d] Coupling was not observable due to rapid solvent exchange. [e] Coupling constant was most readily observed in spectrum containing 1.0 equiv of HMPA. [f] Assignment of chemical shifts to discrete triple ions varying only in the gegenion is arbitrary.
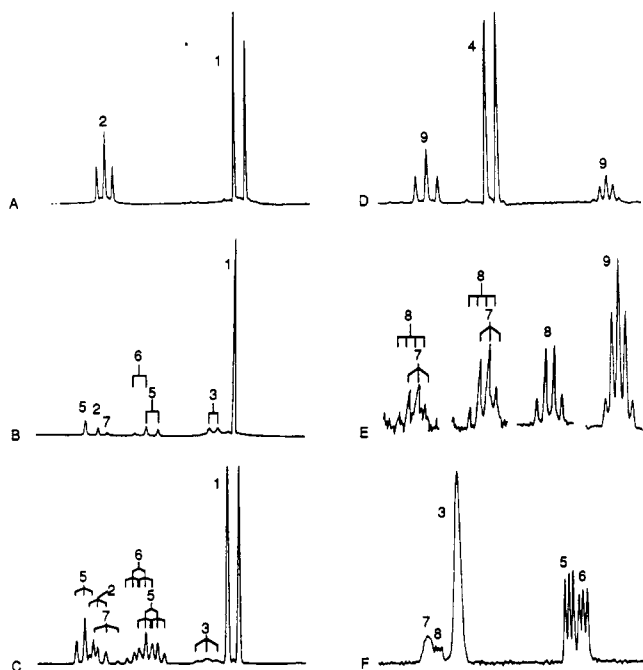

Figure 1. 6Li NMR spectra of 0.13 M LiHMDS in 3:1 THF/pentane at -115 °C. (A) [6Li,15N]LiHMDS with no added HMPA; (B) [6Li]LiHMDS with 0.3 equiv of HMPA/Li; (C) [6Li,15N]LiHMDS with 0.3 equiv of HMPA/Li; (D) [6Li,15N]LiHMDS with 2.0 equiv of HMPA/Li; (E) +LiS$_x$ gegenion 6Li resonance observed with 0.3, 0.8, 1.5, and 2.0 equiv of HMPA/Li, respectively. (F) 31P NMR spectrum of [6Li]LiHMDS with 0.3 equiv of HMPA/Li recorded at -120 °C.

level of spectral quality and complexity; additional spectra are included as supplementary material. The resonance assignments are summarized in Table I. All detectable resonances are reproducible and assigned to discrete species.

Structure of LiHMDS in Toluene and THF/Pentane. [6Li,15N]-LiHMDS was prepared as described in the Experimental Section and subjected to 6Li and 15N NMR spectroscopic analysis (Table I). The peak counts and multiplicities observed for 0.13 M solutions in 3:1 THF/pentane are fully consistent with a mixture of monomer 1 and a cyclic oligomer, as first described by Kimura and Brown (Figures 1A and 2A; Table I).[12] The solvation-state assignment of 1 (and 2) is based on mounting indirect evidence, as outlined in the Discussion. Spectra recorded on a 0.2 M solution of [6Li,15N]LiHMDS in pentane display 6Li and 15N resonances

consistent with approximately equal proportions of two cyclic oligomers. The corresponding spectrum recorded on a 0.2 M toluene solution shows evidence of a single oligomer.[15] This surprising dependence on the nature of the hydrocarbon solvent was noted by Kimura and Brown.

Attempts to distinguish cyclic dimers from higher cyclic oligomers using inverse-detected 15N homonuclear zero-quantum NMR spectroscopy afforded mixed results (Figure 3).[11] The absence of five-line splitting in the f$_1$ (15N) dimension of Figure 3a is nicely consistent with a THF-solvated dimer and inconsistent with trimers or higher oligomers. The 15N zero-quantum spectrum recorded on a 0.2 M solution of [6Li,15N]LiHMDS in toluene at -33 °C also shows no characteristic splitting in f$_1$ (Figure 3B).[15] However, broadening in f$_1$ is both severe and reproducible. (See the corresponding spectrum of the higher oligomer of [6Li,15N]-LiTMP in Figure 3C for comparison). The origin of the broadening in the 15N dimension of Figure 2B remains unclear. It is possible that the single 6Li and 15N resonances in toluene-d_8 correspond to the superposition of resonances from a dimer and higher oligomer, although no evidence of such a mixture was discernible by 6Li, 13C, or 15N NMR spectroscopy. In any event, a clear distinction of dimer from higher oligomers can be made only for the THF solvate at this time.[42]

Structure of LiHMDS in THF/HMPA/Pentane. Addition of HMPA to 0.13 M solutions of [6Li]LiHMDS and [6Li,15N]-LiHMDS in THF/pentane (2:1) causes complex 6Li, 15N, and 31P NMR spectroscopic changes consistent with the structures depicted in Scheme I. Resonance assignments and resonance correlations are listed in Table I. Representative 6Li and 31P NMR spectra are illustrated in Figure 1. The corresponding 15N

(13) For additional structural studies of LiHMDS, see: Wannagat, U. Adv. Inorg. Chem. Radiochem. **1964**, 6, 237. Arnett, E. M.; Moe, K. D. J. Am. Chem. Soc. **1991**, 113, 7288. Rogers, R. D.; Atwood, J. L.; Grüning, R. J. Organomet. Chem. **1978**, 157, 229. Mootz, D.; Zinnius, A.; Böttcher, B. Angew. Chem., Int. Ed. Engl. **1969**, 8, 378. Renaud, P.; Fox, M. A. J. Am. Chem. Soc. **1988**, 110, 5702. Fjeldberg, T.; Lappert, M. F.; Thorne, A. J. J. Mol. Struct. **1984**, 125, 265. Fjeldberg, T.; Hitchcock, P. B.; Lappert, M. F.; Thorne, A. J. J. Chem. Soc., Chem. Commun. **1984**, 822. Engelhardt, L. M.; May, A. S.; Raston, C. L.; White, A. H. J. Chem. Soc., Dalton Trans. **1983**, 1671. Williard, P. G.; Liu, Q.-Y.; Lochmann, L. J. Am. Chem. Soc. **1992**, 114, 348. Lochmann, L.; Trekoval, J. J. Organomet. Chem. **1975**, 99, 329. Nichols, M. A.; Williard, P. G., submitted for publication. Atwood, J. L.; Lappert, M. F.; Leung, W.-P.; Zhang, H., unpublished.

(14) Selected reviews of N-lithiated species: Gregory, K.; Schleyer, P. v. R.; Snaith, R. Adv. Inorg. Chem. **1991**, 37, 47. Mulvey, R. E. Chem. Soc. Rev. **1991**, 20, 167.

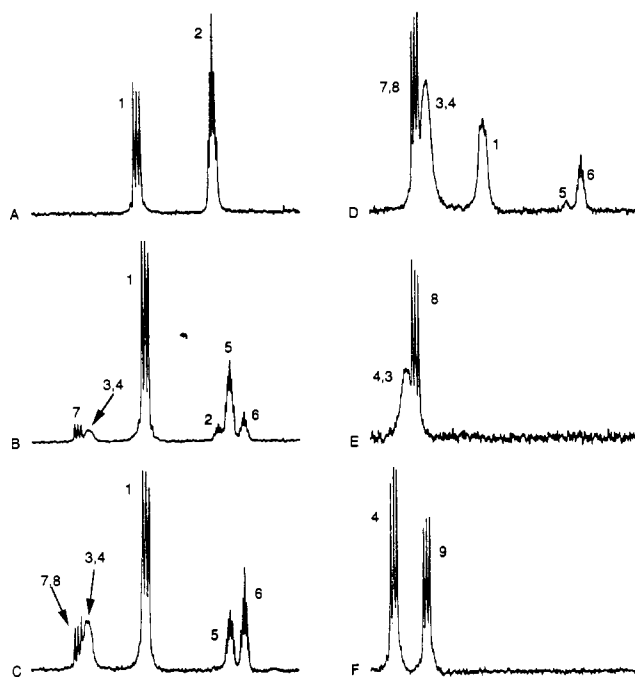(15) Approximately 5% of the second (higher) oligomer can be seen in toluene solution at -90 °C.

Figure 2. $^{15}N\{^1H\}$ NMR spectra of 0.13 M [^{6}Li,^{15}N]LiHMDS in 3:1 THF/pentane at -115 °C. (A) No added HMPA; (B) 0.5 equiv of HMPA/Li; (C) 0.8 equiv of HMPA/Li; (D) 1.0 equiv of HMPA/Li; (E) 1.5 equiv of HMPA/Li; (F) 1.8 equiv of HMPA/Li; (G) 2.0 equiv of HMPA/Li.

NMR spectra illustrated in Figure 2 provide the most visually retrievable view of the structural changes that occur with added HMPA.

Species **1**, **2**, **3**, **5**, **6**, and **7** coexist in the presence of 0.3 equiv of HMPA per Li (Figures 1B and 2B). Incremental addition of HMPA causes serial solvation of the dimer to give mixed solvated dimer **5** and disolvated dimer **6** via somewhat soft equilibria; dimers **2**, **5**, and **6** coexist at 0.3–0.5 equiv of HMPA/Li. The stepwise solvation of the monomer was difficult to follow due to signal averaging of the HMPA solvates **3** and **4** and consequent loss of ^{6}Li–^{31}P coupling as **4** appears. Nevertheless, the HMPA concentration-independent mixture of the disolvated monomer **4** and triple ion **9** at high HMPA concentrations supports the assignment of the limiting monomer as disolvate **4**. Triple ions form even at very low HMPA concentrations. The sequential formation of triple ions **7**, **8**, and **9** is readily detected by monitoring the ^{6}Li resonances of the $^+$LiS$_x$ gegenion (δ –0.69 to –0.54; Figure 1E), as documented by Reich for other dissociated lithium salts.[4,5] Thus, triple ion **7** bearing two HMPA ligands (and presumably two THF ligands) on the Li$^+$ gegenion can be observed with as little as 0.3 equiv of HMPA/Li. At 1.5 equiv of HMPA, triple ion **8** bearing a tris(HMPA)-solvated gegenion is the predominant triple ion form, eventually being replaced by **9** at high ($\geq$2.0 equiv) HMPA concentrations (Figure 1E).

^{6}Li–^{15}N and ^{6}Li–^{31}P Heteronuclear Chemical Shift Correlations. Heteronuclear multiple quantum correlation (HMQC) spectroscopy,[16,17] originally developed for the measurement of ^{1}H–^{13}C and ^{1}H–^{15}N heteronuclear chemical shift correlations, has been used to correlate nonproton nuclei.[17] Of special significance to the work described herein, Günther and co-workers applied ^{6}Li–^{13}C HMQC spectroscopy to the solution structure determinations of some complex dilithiated species.[18] More recently,

the ^{6}Li–^{15}N HMQC spectroscopic method was described.[10] The pulse sequence has been analyzed in detail elsewhere.[16,19,20]

Figure 4 shows the ^{6}Li–^{15}N HMQC spectrum of a 0.2 M solution of [^{6}Li,^{15}N]LiHMDS in THF/pentane (3:1) containing 0.3 equiv of HMPA (per Li) at -115 °C. As noted previously,[11] the center lines of ^{15}N coupled triplets correspond to nonselected orders of coherence and are canceled by the phase cycle. The -1:0:1 intensity pattern (1:0:1 in the magnitude mode display) takes on the appearance of a widely spaced doublet in the two-dimensional spectrum, as exemplified by the cross peak corresponding to triple ions **7/8** (arrow A in Figure 4). The cross peaks for lithium atoms in a ^{6}Li(^{15}N)$_2$(^{31}P) spin system appear as -1:0:1 ^{15}N coupling patterns further split by the ^{31}P spin. The

(19) Müller, L. *J. Am. Chem. Soc.* **1979**, *101*, 4481.

(20) The application of the HMQC sequence to IS$_n$ spin systems ($n > 1$) has been discussed previously: Nanz, D.; von Philipsborn, W. *J. Magn. Reson.* **1991**, *92*, 560. For related examples, see Frey, M. H.; Wagner, G.; Vašák, M.; Sørensen, O. W.; Neuhaus, D.; Wörgötter; Kägi, J. H. R.; Ernst, R. R.; Wüthrich, K. *J. Am. Chem. Soc.* **1985**, *107*, 6847. Otvos, J. D.; Engseth, H. R.; Wehrli, S. R. *J. Magn. Reson.* **1985**, *61*, 579. Live, D.; Armitage, I. M.; Dalgarno, D. C.; Cowburn, D. *J. Am. Chem. Soc.* **1985**, *107*, 1775.

(21) Stewart, J. J. P. *QCPE* 581.

(22) Thiel, W.; Clark, T., unpublished results.

(23) Romesberg, F. E.; Collum, D. B. *J. Am. Chem. Soc.* **1992**, *114*, 2112.

(24) Bernstein, M. P.; Romesberg, F. E.; Fuller, D. J.; Harrison, A. T.; Collum, D. B.; Liu, Q.-Y.; Williard, P. G. *J. Am. Chem. Soc.* **1992**, *114*, 5100.

(25) Galiano-Roth, A. S.; Collum, D. B. *J. Am. Chem. Soc.* **1989**, *111*, 6772.

(26) Galiano-Roth, A. S.; Michaelides, E. M.; Collum, D. B. *J. Am. Chem. Soc.* **1988**, *110*, 2658.

(27) Jackman, L. M.; Scarmoutzos, L. M.; DeBrosse, C. W. *J. Am. Chem. Soc.* **1987**, *109*, 5355. Depue, J. S.; Collum, D. B. *J. Am. Chem. Soc.* **1988**, *110*, 5518. Kallman, N.; Collum, D. B. *J. Am. Chem. Soc.* **1987**, *109*, 7466. Wanat, R. A.; Collum, D. B.; Van Duyne, G.; Clardy, J.; DePue, R. T. *J. Am. Chem. Soc.* **1986**, *108*, 3416.

(28) Quantitative spectroscopic studies of the LiHMDS monomer–dimer equilibrium in THF–TMEDA mixtures appear to be most consistent with a model based upon monomer **1**, a mixed solvated monomer, and dimer **2** as the predominant THF-solvated forms: Bernstein, M. P.; Collum, D. B., unpublished.

(29) Lithium bis(2-adamantyl)amide forms exclusively disolvated monomer in the presence of $\geq$2.0 equiv of HMPA per Li. Sakuma, K.; Romesberg, F. E.; Cajthaml, C. E.; Collum, D. B., unpublished.

(30) Fuoss, R. M.; Kraus, C. A. *J. Am. Chem. Soc.* **1933**, *55*, 2387.

(31) Fraenkel, G.; Hallden-Abberton, M. P. *J. Am. Chem. Soc.* **1981**, *103*, 5657.

(32) Jackman, L. M.; Scarmoutzos, L. M.; Porter, W. *J. Am. Chem. Soc.* **1987**, *109*, 6524. Jackman, L. M.; Scarmoutzos, L. M.; Smith, B. D.; Williard, P. G. *J. Am. Chem. Soc.* **1988**, *110*, 6058.

(33) Vinogradova, L. V.; Zgonnik, V. N.; Nikolaev, N. I.; Tsvetanov, K. B. *Eur. Polym. J.* **1979**, *15*, 545. Arnett, E. M.; Maroldo, S. G.; Schriver, G. W.; Schilling, S. L.; Troughton, E. B. *J. Am. Chem. Soc.* **1985**, *107*, 2091. Cambillau, C.; Bram, G.; Corset, J.; Riche, C. *Nouv. J. Chim.* **1979**, *3*, 9. Cambillau, C.; Ourevitch, M. *J. Chem. Soc., Chem. Commun.* **1981**, 996. Raban, M.; Noe, E. A.; Yamamoto, G. *J. Am. Chem. Soc.* **1977**, *99*, 6527. Olmstead, W. N.; Bordwell, F. G. *J. Org. Chem.* **1980**, *45*, 3299. Teixidor, F.; Llobet, A.; Casabo, J.; Solans, X.; Font-Altaba, M.; Aguilo, M. *Inorg. Chem.* **1985**, *24*, 2315. Tsvetanov, Ch. B.; Dotcheva, D. T. *J. Polym. Sci., Polym. Chem.* **1986**, *24*, 2253. Buttrus, N. H.; Eaborn, C.; Hitchcock, P. B.; Smith, J. D.; Stamper, J. G.; Sullivan, A. C. *J. Chem. Soc., Chem. Commun.* **1986**, 969. Eaborn, C.; Hitchcock, P. B.; Smith, P. B.; Sullivan, A. C. *J. Chem. Soc., Chem. Commun.* **1983**, 827. Viteva, L.; Stefanovsky, Y.; Tsvetanov, C.; Gorrichon, L. *J. Phys. Org. Chem.* **1990**, *3*, 205. Hertkorn, N.; Köhler, F. H. *Z. Naturforsch. B* **1990**, *45*, 848. Bauer, W.; O'Doherty, G. A.; Schleyer, P. v. R.; Paquette, L. A. *J. Am. Chem. Soc.* **1991**, *113*, 7093. Arnold, J. *J. Chem. Soc., Chem. Commun.* **1990**, 976. Eirmann, M.; Hafner, K. *J. Am. Chem. Soc.* **1992**, *114*, 135. Strohmeier, W.; Landsfeld, H.; Gernert, R. *Z. Elektrochem.* **1962**, *66*, 823.

(34) Seebach, D. *Angew. Chem., Int. Ed. Engl.* **1988**, *27*, 1624. Galiano-Roth, A. S.; Collum, D. B. *J. Am. Chem. Soc.* **1988**, *110*, 3546. Bhattacharyya, D. N.; Lee, C. L.; Smid, J.; Szwarc, M. *J. Phys. Chem.* **1965**, *69*, 612. Bhattacharyya, D. N.; Smid, J.; Szwarc, M. *J. Am. Chem. Soc.* **1964**, *86*, 5024.

(35) Richey, H. G., Jr.; Farkas, J., Jr. *Organometallics* **1990**, *9*, 1778. Fabicon, R. M.; Parvez, M.; Richey, H. G., Jr. *J. Am. Chem. Soc.* **1991**, *113*, 1412. Corey, E. J.; Hannon, F. J. *Tetrahedron Lett.* **1987**, *28*, 5233. Corriu, R. *Pure Appl. Chem.* **1988**, *60*, 99. Pelter, A.; Smith, K. In *Comprehensive Organic Chemistry*; Barton, D. H. R., Ollis, W. D., Eds.; Pergamon Press: New York, 1979; Vol. 3, Chapter 14. Lipshutz, B. H. *Synthesis* **1987**, 325.

(36) Frost, A. A.; Pearson, R. G. *Kinetics and Mechanism*, 2nd ed.; Wiley: New York, 1953, p 125.

(37) Kim, Y.-J.; Bernstein, M. P.; Galiano-Roth, A. S.; Romesberg, F. E.; Williard, P. G.; Fuller, D. J.; Harrison, A. T.; Collum, D. B. *J. Org. Chem.* **1991**, *56*, 4435.

(38) Lewis, H. L.; Brown, T. L. *J. Am. Chem. Soc.* **1970**, *92*, 4664.

(39) Kofron, W. G.; Baclawski, L. M. *J. Org. Chem.* **1976**, *41*, 1879.

(16) Bax, A.; Griffey, R. H.; Hawkins, B. L. *J. Magn. Reson.* **1983**, *55*, 301. Bendall, M. R.; Pegg, D. T.; Doddrell, D. M. *J. Magn. Reson.* **1983**, *52*, 81.

(17) Bodenhausen, G.; Ruben, D. J. *Chem. Phys. Lett.* **1980**, *69*, 185.

(18) Moskau, D.; Brauers, F.; Günther, H.; Maercker, A. *J. Am. Chem. Soc.* **1987**, *109*, 5532.
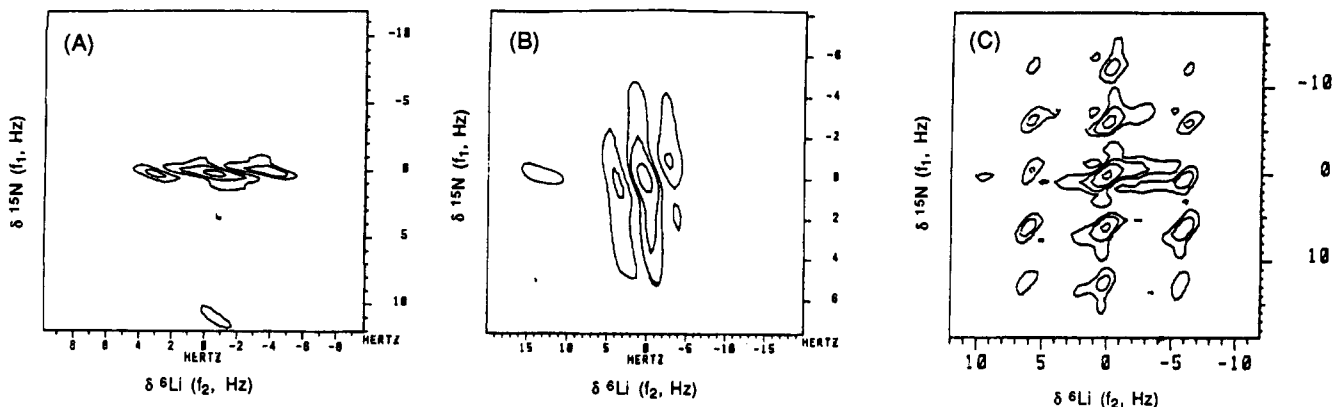
Figure 3. ^{6}Li-detected ^{15}N zero-quantum NMR spectra. (A) 0.2 M [^{6}Li,^{15}N]LiHMDS in 2:3 THF/pentane at –115 °C; (B) 0.2 M [^{6}Li,^{15}N]LiHMDS in toluene at –33 °C; (C) 0.25 M [^{6}Li,^{15}N]LiTMP (higher oligomer) in benzene at 30 °C taken from ref 11 for comparison. Data were processed in phase-sensitive mode. Traces A–C show the 1:–2:1 coupling pattern in the f_2 (^{6}Li) dimension. Traces A and C show the absence and presence, respectively, of splitting in the f_1 (^{15}N zero-quantum) dimension. Digital resolution in f_1 prior to zero filling is 0.50 Hz for A and 0.69 Hz for B. Spectra were recorded on a Bruker AC 300 spectrometer operating at 44.17 and 30.42 MHz for ^{6}Li and ^{15}N, respectively.

Scheme I
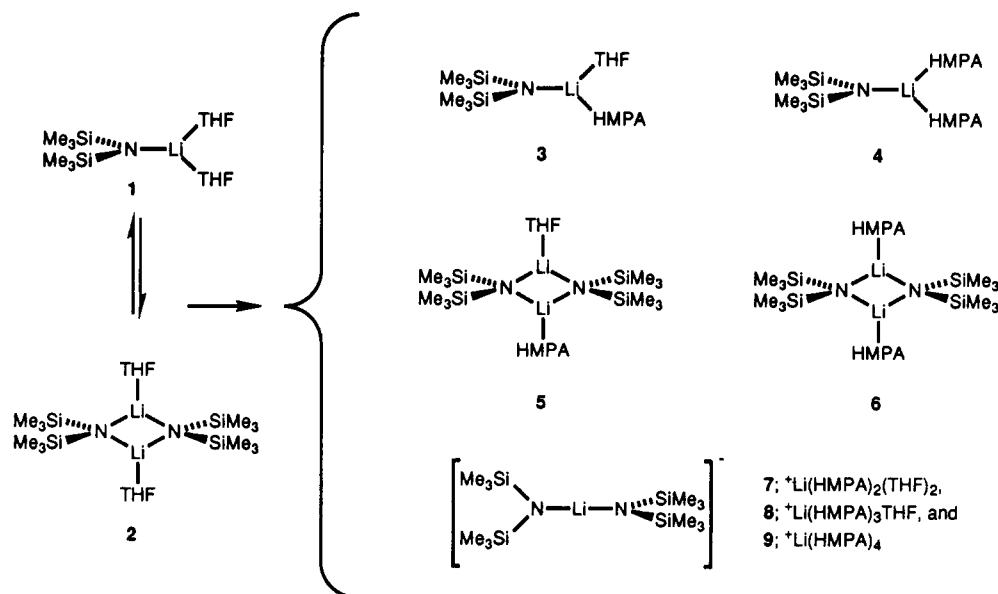
HMPA-solvated lithium atoms in **5** and **6** (arrow B in Figure 4) display the coupling patterns expected when J_{P-Li} is nearly (but not quite) twice the magnitude of J_{N-Li} (Figure 5). Overall, the superposition of ^{6}Li–^{31}P and ^{6}Li–^{15}N coupling affords a spectral complexity that is more readily resolved by ^{6}Li–^{15}N HMQC spectroscopy than by the more conventional single frequency decoupling methods.[40] We add, however, that the optimal confidence in the structure assignments comes from a combination of the one- and two-dimensional methods using both [^{6}Li]-LiHMDS and [^{6}Li,^{15}N]LiHMDS.

The ^{31}P triplets observed for the LiHMDS–HMPA solvates are markedly sharper than those observed for LiTMP.[7] This allowed us to determine the ^{6}Li–^{31}P resonance correlations[6] listed in Table I using ^{31}P–^{6}Li HMQC spectroscopy. In the ^{31}P–^{6}Li HMQC spectroscopic analyses, we employed the same pulse sequence as in the ^{6}Li–^{15}N correlation experiment.[10,17] However, detection of the nucleus having a higher gyromagnetic ratio (^{31}P in this case) affords greater sensitivity. Favorable ^{31}P relaxation times ($T_1 = 0.8$–1.0 s) relative to the corresponding ^{6}Li T_1 values (up to 20 s) also makes direct ^{31}P detection desirable. A ^{31}P–^{6}Li

HMQC spectrum recorded at –120 °C on a 0.2 M solution of [^{6}Li]LiHMDS containing 0.3 equiv of HMPA is illustrated in Figure 6. The ^{6}Li–^{31}P couplings are not resolved in the one-dimensional ^{31}P resonances corresponding to monomers **3** and **4**, but the coupling is resolved in the ^{6}Li resonance of **3** at high field (at 58.84 MHz) and low HMPA concentrations. The observed cross peaks and the HMPA concentration dependencies in the ^{31}P and ^{6}Li one-dimensional spectra are consistent with the Li–P connectivities proposed for **3** and **4**.

MNDO Calculations. The heats of formation of various structural forms of LiHMDS calculated with MNDO (MO-PAC[21,22]) are listed in Table II. The relative heats of formation are summarized in Scheme II. The heats of dimerization of LiHMDS are listed in Table III along with previously reported results for three dialkylamides for comparisons. Relative heats of oligomerization are shown in Scheme III. All energies quoted are normalized to a *per lithium* basis (kcal/mol per Li) and refer only to enthalpies to the exclusion of entropic effects.

The optimized geometries proved to be similar to those reported for LDA and LiTMP previously.[23,24] The planes defined by the O–Li–O solvation linkages and the Si–N–Si linkages in the

(40) Gilchrist, J. H.; Harrison, A. T.; Fuller, D. J.; Collum, D. B. *J. Am. Chem. Soc.* **1990**, *112*, 4069.

(41) Chandrakumar, N. *J. Magn. Reson.* **1984**, *60*, 28.

(42) **Note Added in Proof:** Recent improvements in the ^{15}N zero-quantum NMR spectroscopic method reveal that the [^{6}Li,^{15}N]LiHMDS cyclic observed in toluene-d_8 is indeed a dimer. These results will be described in due course.
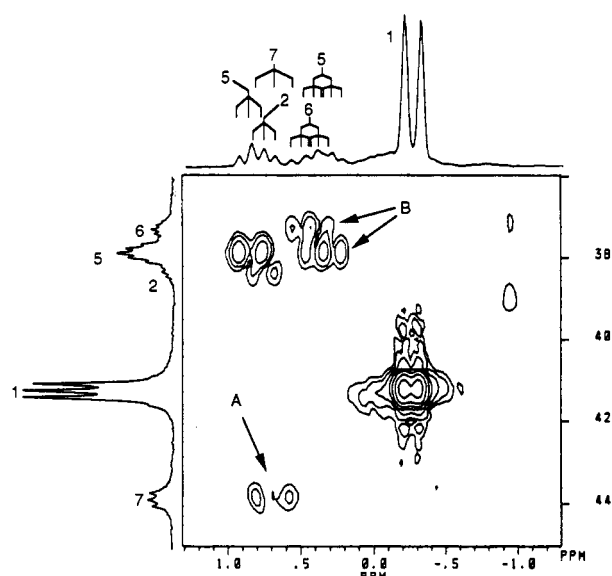
Structure of LiHMDS in the Presence of HMPA

J. Am. Chem. Soc., Vol. 115, No. 9, 1993 3479

Figure 4. ^{6}Li–^{15}N HMQC spectrum of 0.2 M [^{6}Li,^{15}N]LiHMDS with 0.3 equiv of HMPA/Li in 3:1 THF/pentane at –115 °C. The 32 t_1 increments were acquired with 256 transients/increment. The upper and left-hand traces are the corresponding one-dimensional ^{6}Li and ^{15}N{^{1}H}NMR spectra, respectively.

monomer are roughly perpendicular (Figure 7). The optimized dimers show geometries that are normal as deemed by comparisons with available crystal structures (Figure 8).[14] The triple ions show a linear N–Li–N fragment with the two planes defined by the Si–N–Si fragments rotated approximately 90° (Figure 9), presumably to minimize transannular interactions and to maintain overlap of the lone pairs on the two nitrogens with the two empty p orbitals on lithium.

As noted for other lithium dialkylamides,[23] the MNDO calculations suggest that lithium amide dimerization is promoted by the high steric demands of placing two solvents per lithium on the monomers. Substitution of HMPA for THF causes disproportionate stabilization of monomers relative to dimers. The stabilization arising from the large dipole moment of HMPA appears to offset the steric demands. One should note, however, that little *net* deaggregation is observed experimentally due to the intervention of highly stable triple ions (vide infra).

The heats of formation and selected geometrical parameters for LiHMDS open dimers and triple ions are listed in Table IV. The relative enthalpies associated with conversion of cyclic dimers

to open dimers, ion-paired triple ions, and fully ionized triple ions (Scheme IV) are listed in Table V. The results from previous studies of LDA and LiTMP are included for comparison. The propensity to form open dimers is sensitive to the substituents on nitrogen following the order LDA < LiHMDS < LiTMP. Substitution of HMPA for THF further stabilizes open dimers relative to cyclic dimers by approximately 2 kcal/mol per Li for all of the amides.

As seen in the formation of open dimers, the propensity to form triple ions from cyclic dimers follows the order LDA < LiHMDS < LiTMP. The added stabilization by substitution of HMPA for THF is insensitive to the substituents on nitrogen (approximately 5 kcal/mol per Li). One should note that the absence of d-type orbital functions may cause MNDO to underestimate charge stabilization on the [(Me$_3$Si)$_2$N-Li-N-(SiMe$_3$)$_2$]$^-$ fragment (such as through back-bonding). Moreover, we feel that the high propensities of LiTMP and LiHMDS to form triple ions derive from substantially different influences. The experimentally observable LiHMDS triple ions may arise from a substantial charge stabilization, whereas previous computational studies suggest that the driving force for formation of (experimentally observable) LiTMP triple ions is the relief of severe steric strain in the cyclic dimers.[23] In this context, it is instructive to compare the change in enthalpy of relatively unhindered, isostructural lithiated silylamides and dialkylamides (eqs 1 and 2). Even without inclusion of possible charge

$$(1)$$

$$(2)$$
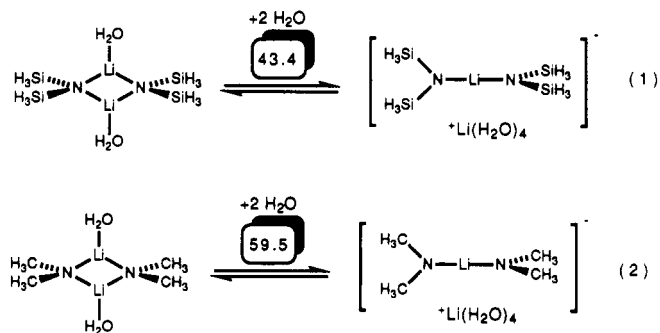
stabilization by d-type orbitals on silicon, the silylamide shows a 16 kcal/mol per Li greater propensity to form triple ions than does the carbon analog.

Discussion

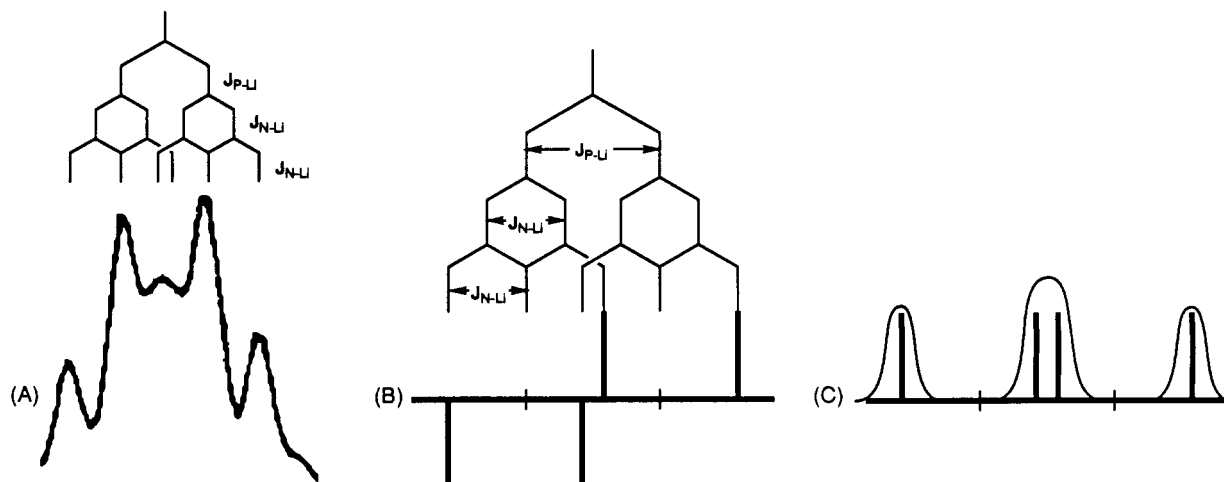In 1971, Kimura and Brown reported ^{1}H and ^{7}Li NMR spectroscopic and colligative studies of LiHMDS.[12] They

Figure 5. (A) ^{6}Li resonance of [^{6}Li,^{15}N]6 from a spectrum of a 0.13 M solution [^{6}Li,^{15}N]LiHMDS containing 1.0 equiv of HMPA per Li. (B) Stick representation of the cross-peak splitting in a ^{6}Li(^{15}N)$_2$(^{31}P) system. Single quantum ^{15}N chemical shift selection produces a –1:0:1 ^{15}N coupling pattern that is further split by the ^{31}P spin. (C) Magnitude mode display of (B).

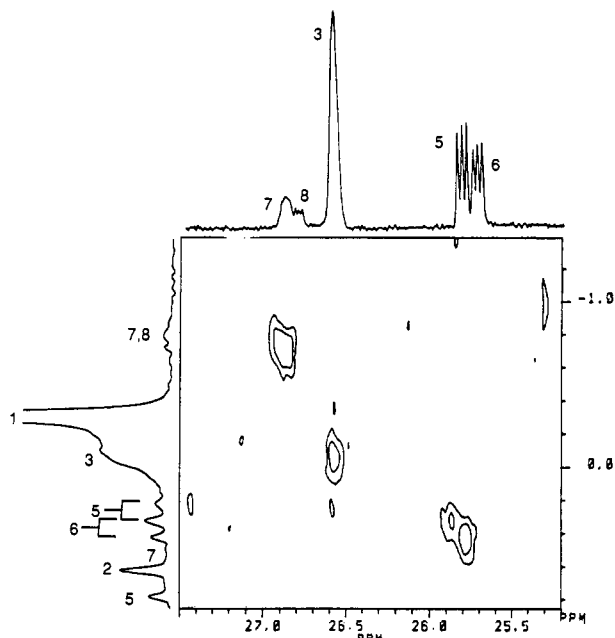**Figure 6.** ^{31}P–^{6}Li HMQC spectrum of 0.2 M [^{6}Li]LiHMDS with 0.3 equiv of HMPA in 3:1 THF/pentane at –120 °C. The 32 t_1 increments were acquired with 512 transients/increment. The upper and left-hand traces correspond to one-dimensional ^{31}P{^{1}H} and ^{6}Li NMR spectra, respectively. The one-dimensional ^{31}P spectrum was recorded at 161.82 MHz on a Varian XL-400 spectrometer. The ^{6}Li spectrum and ^{31}P–^{6}Li HMQC spectra were recorded on a Bruker AF-300 spectrometer.

concluded that LiHMDS exists as a concentration-dependent mixture of dimer and tetramer in pentane and as a mixture of monomer and dimer in THF. The ^{6}Li and ^{15}N NMR spectroscopic studies of [^{6}Li,^{15}N]LiHMDS described above are consistent with Kimura and Brown's conclusions in every respect. The resonance multiplicities clearly differentiate monomers from cyclic oligomers. ^{15}N homonuclear zero-quantum NMR spectroscopy[11] affords further distinction of the THF-solvated cyclic dimer from the higher cyclic oligomers. The success of Kimura and Brown's early investigations is remarkable considering the instrumentation available at the time.[42]
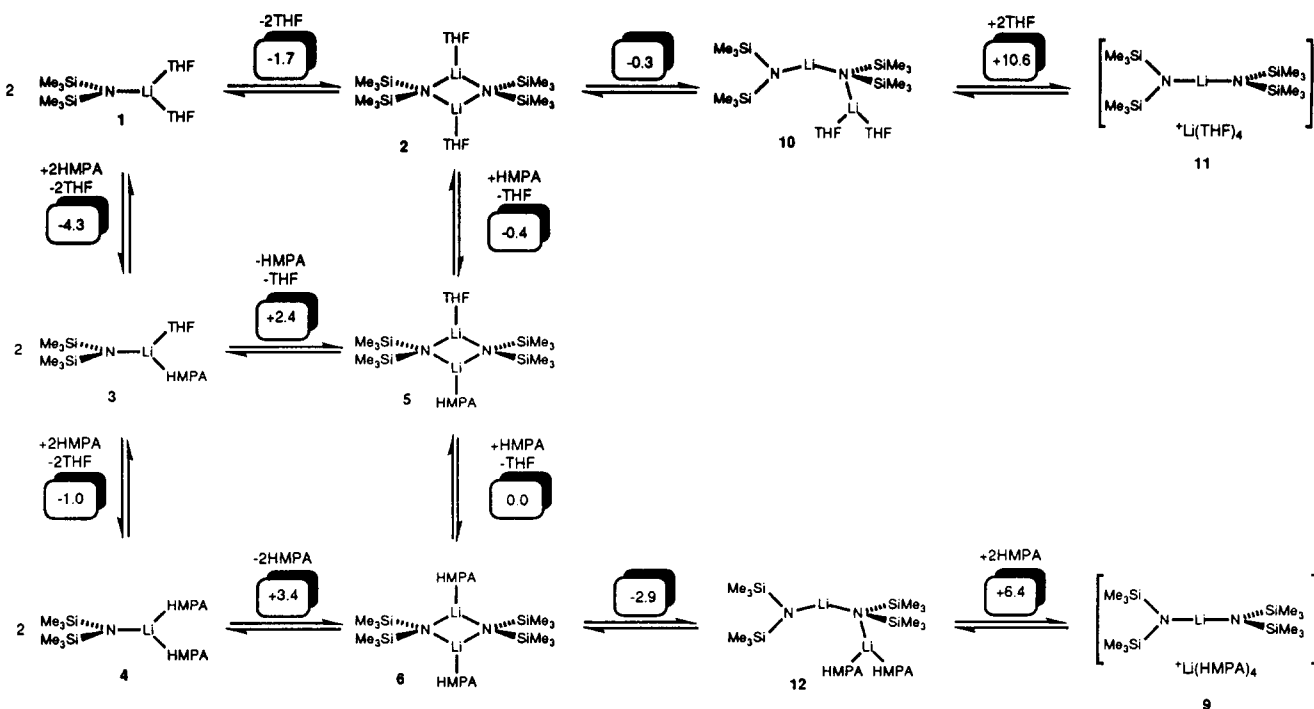
Table II. Heats of Formation of Solvated Lithium Hexamethyldisilazide[a]

	(LiHMDS)$_1$	(LiHMDS)$_2$
unsolvated	–125.7	–298.9
H$_2$O	–201.1	–355.9
2H$_2$O	–270.0	–415.6
3H$_2$O	–329.1	
Me$_2$O	–188.7	–340.1
2Me$_2$O	–240.8	–382.0
THF	–196.1	
2THF	–257.0	–398.8
2HMPA	–212.5	–349.3
THF/HMPA	–236.4	–374.2

[a] Enthalpies are reported in kcal/mol. *Relative* heats of formation in subsequent tables are listed on a per lithium basis (kcal/mol per Li). The heats of formation (kcal/mol) of the donor solvents are as follows: H$_2$O, –60.9; Me$_2$O, –51.2; THF, –59.3; HMPA, –34.4.

Table III. Heats of Dimerization ($\Delta H°$) of Lithium Amides[a]
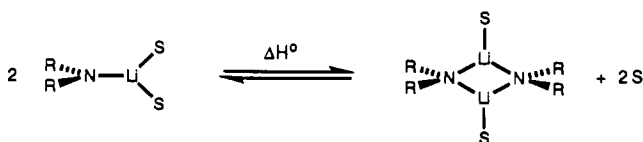
	unsolvated	S = H$_2$O	S = Me$_2$O	S = THF	S = HMPA
LiHMDS	–23.8	1.3	–1.4	–1.7	3.4
Me$_2$NLi	–35.1	–9.8	–12.0	–12.4	–8.3
LDA	–24.4	–3.0	–4.0	–4.7	–1.1
LiTMP	–18.4	3.2	3.3	0.6	5.0

[a] Enthalpies are listed on a per lithium basis (kcal/mol per Li).

^{6}Li, ^{15}N, and ^{31}P NMR spectroscopic investigations of [^{6}Li,^{15}N]-LiHMDS in THF containing variable concentrations of HMPA reveal complex aggregation and solvation equilibria, summarized in Scheme I. ^{6}Li–^{15}N HMQC and ^{31}P–^{6}Li HMQC spectroscopies provide Li–N and Li–P resonance correlations that are essential to the deconvolution of such complex equilibria. Both the monomer and the dimer undergo serial solvation by HMPA. In addition, triple ion **7** appears at very low concentrations of HMPA (0.3–0.5 equiv), with serial solvation of the $^+$Li gegenion observable with increasing HMPA concentrations. In the limit of excess

Scheme II

Scheme III
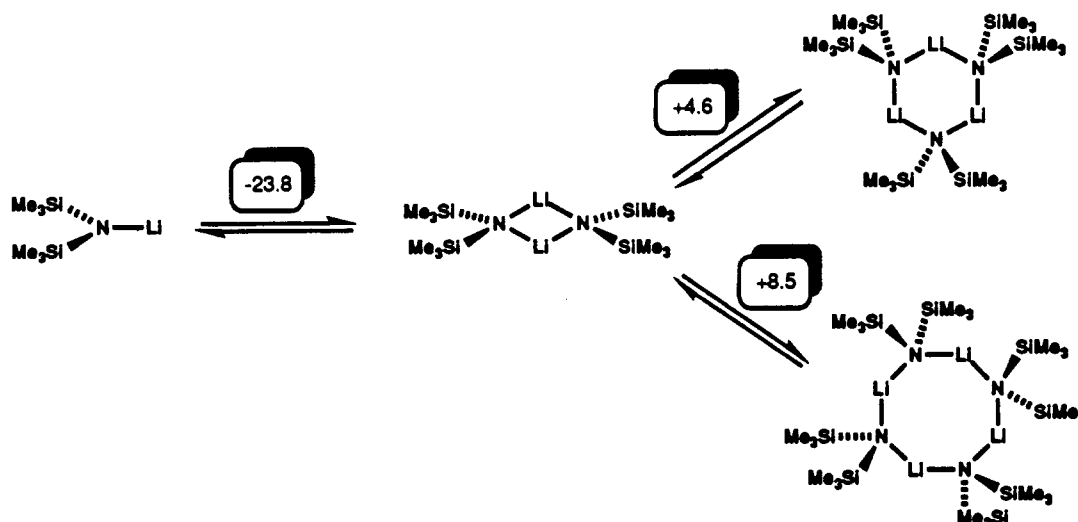
HMPA, an approximate 2:1 mixture of monomer **4** and triple ion **9** coexist to the exclusion of cyclic dimers.

Although Kimura and Brown clearly demonstrated that the species assigned as the LiHMDS monomer in THF is at a higher per lithium solvation state than the dimer,[12] depiction of **1** and **2** as disolvates is based somewhat speculatively upon mounting indirect evidence[7,23-29] including: (1) analogies with the corresponding HMPA solvates of LiHMDS and related lithium dialkylamides,[7,29] (2) computational studies of LiHMDS (see Results and below) and related dialkylamides,[23,24,29] and (3) solvation studies of sterically hindered lithium anilides.[27] We add, however, that a slight THF-concentration-dependent chemical shift of the LiHMDS monomer in THF/toluene mixtures[12,28] could be construed as evidence of multiple solvation states.

Comparison of the LiHMDS–HMPA solvates with structures of lithium 2,2,6,6-tetramethylpiperidide (LiTMP) solvated by HMPA described previously[7] reveals strong parallels. Both amides exist as monomer–dimer mixtures in neat THF and undergo serial solvation of monomers, dimers, and triple ions with added HMPA. The primary difference between LiHMDS and LiTMP is that LiTMP forms an open dimer (**13**) in place of disolvated triple ion **14**. In contrast, LiHMDS triple ion **7** is formed to the exclusion of open dimer **15**. The greater anion-

13; R₂N = TMP
15; R₂N = (Me₃Si)₂N

7; R₂N = (Me₃Si)₂N
14; R₂N = TMP
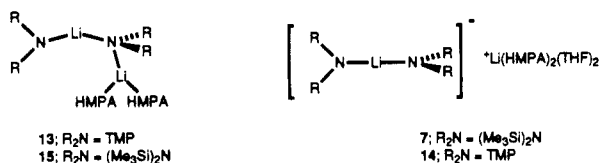
stabilizing capacity of the (Me₃Si)₂N⁻ fragment appears to promote the charge separation. Overall, despite the deep-seated structural changes that occur upon addition of HMPA, *HMPA does not substantially deaggregate either LiHMDS or LiTMP.*[7]

Although triple ions have been mentioned as early as 1933,[30] they are still cited only rarely in the organolithium literature.[31-34] Fraenkel and Hallden-Abberton described the first well-characterized example in 1981.[31] More recently, Jackman and co-workers found that treatment of hindered lithium anilides with excess HMPA affords a mixture of monomer and triple ion.[32] They astutely noted that strong donor solvents often said to promote deaggregation will promote triple ion formation as well. Analogy with other main group "ate" complexes[35] suggests that triple ions may be extremely reactive and more important than previously thought. However, a clear demonstration of the kinetic consequences of triple ion formation remains elusive.[34]

MNDO Calculations: Correlation of Theory with Experiment. In principle, a comparison of theory with experiment would logically begin with the calculated enthalpy of dimerization ($\Delta H°$ = +1.0 kcal/mol per Li for conversion of **1** to **2**) and the experimental value (−2.0 kcal/mol per Li) determined by Kimura and Brown.[12] However, MNDO calculations provide enthalpies in the gas phase at 25 °C. The solution- and gas-phase enthalpies are related according to eq 3. Using the known heat of

$$\Delta H°(\text{solution}) = \Delta H°(\text{gas}) - \sum \Delta H°(\text{vaporization}) \quad (3)$$

vaporization of THF (7.1 kcal/mol), the calculated and observed heats of dimerization for LiHMDS in THF agree *if* the heat of vaporization of the monomer less half that of the dimer is approximately 5 kcal/mol per Li. Although this is in line with comparisons of monomers and dimers of more standard organic molecules,[36] the absence of heats of vaporization renders a quantitative theory–experiment comparison impossible.

A second problem associated with standard states arises when one attempts to use MNDO to provide insight into free energies. Free energy differences ($\Delta G°$) and relative free energy differences ($\Delta\Delta G°$) are available by inclusion of the various entropic considerations. However, it is neither valid nor constructive to compare free energies for reactions of different molecularities (whether calculated or measured) due to the standard-state dependence of the entropy component. If, for the sake of discussion, we are willing to ignore mass action effects and other entropic contributions, we can still get some intuition about the behavior of lithium amides in solution from the calculated enthalpies. For example, MNDO predicts that solvent-free LiHMDS exists as a mixture of cyclic dimer and higher oligomers (Scheme III) with decreasing stability correlating with increasing oligomer size. This contrasts in a qualitative sense with the results of colligative studies showing the stability order to be dimer > tetramer > trimer.

In general, however, we avoid many of the problems associated with concentration dependencies by comparing reactions of equal molecularities. In doing so, most entropy contributions cancel (including the concentration dependencies associated with mass action effects). In turn, the $\Delta\Delta H°$ values represent reasonable approximations of relative free energies that are of predictive value. For example, MNDO reproduces the quantitative (stepwise) solvation of the monomer and more gradual solvation of the dimer quite well. Moreover, neither the spectroscopic nor the computational studies provide evidence of stable trisolvated monomers or tetrasolvated dimers. The increasing relative

3482 *J. Am. Chem. Soc., Vol. 115, No. 9, 1993*

Romesberg et al.

Figure 7. Optimized structure of the bis(THF)-solvated LiHMDS monomer **1** as calculated by MNDO.
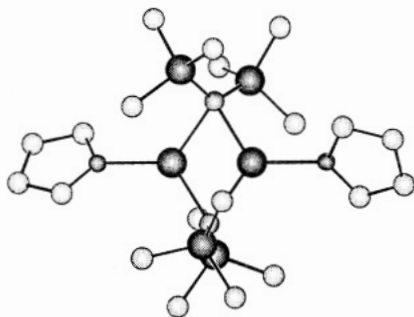

Figure 8. Optimized structure of the mono(THF)-solvated LiHMDS dimer **2** as calculated by MNDO.
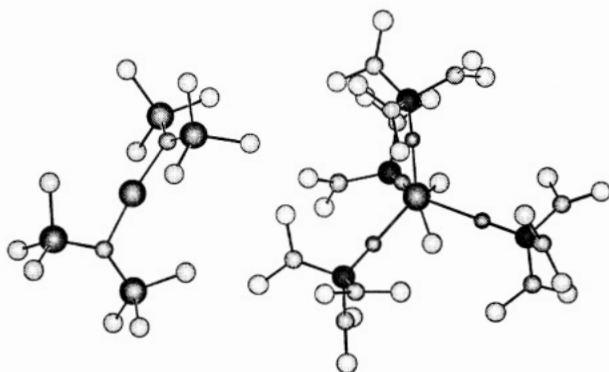

Figure 9. Optimized structure of the tetrakis(HMPA)-solvated LiHMDS triple ion **9** as calculated by MNDO.

stabilization of monomers with substitution of THF by HMPA is consistent with the notion that high solvation energy promotes deaggregation. However, formation of ionized dimers—triple ions **7**, **8**, and **9**—precludes the *net* deaggregation of LiHMDS. The calculations correctly predict that the THF-solvated triple ion **11** is not sufficiently stable to be observed. They also predict that HMPA should confer relative stabilization to triple ion **9**, yet fall short of predicting **9** to be observable.

We also find comparisons of LiHMDS with assorted lithium dialkylamides studied previously[23] to be instructive (Tables III and V). LDA and Me$_2$NLi show a dominance of cyclic dimers irrespective of the number and type of coordinated solvents. In contrast, open dimers and triple ions derived from LiHMDS and LiTMP are quite plausible with THF ligands. The added stabilization of open dimers and triple ions (relative to cyclic dimers) afforded by HMPA coordination is relatively insensitive to the substituents on nitrogen. We hasten to add, however, that we attribute the strikingly similar behavior of LiHMDS and LiTMP to different origins. For LiHMDS, significant charge stabilization by the silicons appears to facilitate the fragmentation leading to triple ions. In contrast, previous results suggest that the relief of steric strain in the highly congested LiTMP cyclic dimers provides the driving force for formation of open dimers and triple ions.

Conclusions

A combination of one- and two-dimensional ^{6}Li and ^{15}N NMR spectroscopic studies of [^{6}Li]LiHMDS and [^{6}Li,^{15}N]LiHMDS affords the following results and conclusions.

(1) The original studies of LiHMDS by Kimura and Brown[12] are correct in every respect. LiHMDS is a monomer–dimer mixture in THF and mixture of oligomers in hydrocarbon solutions.

(2) Incremental addition of HMPA to LiHMDS in THF affords complex structure changes including serial solvation of the monomer and dimer as well as formation and serial solvation of triple ions.

(3) LiHMDS and LiTMP show striking parallels. Both are a mixture of two cyclic oligomers in hydrocarbon solution and a monomer–dimer mixture in THF. Both undergo serial solvation of the monomer and dimer forms as well as afford triple ions and monomers in the limit of excess HMPA. They differ in that LiTMP forms an open dimer under conditions that afford a LiHMDS bis(HMPA)-solvated triple ion.

(4) As seen previously for LiTMP,[7] *addition of HMPA to LiHMDS has little effect on the overall aggregation state.*

(5) Semiempirical (MNDO) calculations have predictive value in the context of even these inordinately complex equilibria.

Experimental Section

Reagents and Solvents. THF and all hydrocarbons were distilled by vacuum transfer from blue or purple solutions containing sodium benzophenone ketyl. The hydrocarbon stills contained 1% tetraglyme to dissolve the ketyl. ^{6}Li metal (95.5% enriched) was obtained from Oak Ridge National Laboratory. The [^{6}Li]ethyllithium used to prepare the ^{6}Li-labeled LiHMDS was prepared and purified by the standard literature procedure.[37,38] The [^{6}Li]LiHMDS and [^{6}Li,^{15}N]LiHMDS were isolated as analytically pure solids as described below. The diphenylacetic acid used to check solution titers[39] was recrystallized from methanol and sublimed at 120 °C under full vacuum. Air- and moisture-sensitive materials were manipulated under argon or nitrogen using standard glovebox, vacuum line, and syringe techniques.

[^{15}N]Hexamethyldisilazane. A nitrogen-flushed 250-mL bomb reaction flask was charged sequentially with [^{15}N]NH$_4$Cl (3.0 g, 55 mmol), 1-(trimethylsilyl)imidazole (24.2 mL, 165 mmol), dimethylethylamine (60 mL), and decane (1.07 mL, internal GC std.). After 6 days of rapid stirring at 60 °C, the reaction was judged to be complete by GC analysis. Solid precipitates caused by pentane addition were filtered off. The volatiles were vacuum transferred, leaving a residual black tar. (The vacuum transfer is necessary to avoid decomposition in the subsequent distillation.) Distillation under reduced pressure (50 Torr) afforded 4.8 g (54% yield based on [^{15}N]NH$_4$Cl) of pure material. Spectral data are consistent with those of commercial material.

[^{6}Li,^{15}N]LiHMDS. A 250-mL round-bottom flask was charged sequentially with doubly recrystallized, doubly sublimed [^{6}Li]ethyllithium (951 mg, 28.5 mmol) and degassed dry pentane (250 mL). Following heating to dissolve the ethyllithium, [^{15}N]hexamethyldisilazane (4.8 g, 29.8 mmol, 1.05 equiv) was added in one portion by gas-tight syringe. The solution was stirred for 10 h at room temperature, at which time it was filtered to remove trace solid residue. After the solution was cooled in an ice bath, the resulting white solid was isolated by filtration, redissolved, and recrystallized from fresh pentane. The yield of pure material is 3.41 g (72%). Pertinent NMR data are listed in Table I.

NMR Spectroscopic Analyses. Samples for spectroscopic analyses were prepared from isotopically labeled LiHMDS using a sample preparation protocol described in detail elsewhere.[7,9] Standard ^{6}Li, ^{15}N, and ^{31}P NMR spectra were recorded on a Varian XL-400 spectrometer operating at 58.84, 40.52, and 161.82 MHz, respectively, and referenced to, respectively, 0.3 M [^{6}Li]LiCl/MeOH at –100 °C (0 ppm), [^{15}N]aniline at –100 °C (52 ppm), and an external sample of HMPA at –100 °C (26.4 ppm).[5,9]

The ^{6}Li–^{15}N HMQC spectra were recorded on a Bruker AC-300 spectrometer using the pulse sequence[16] $90^\circ_X(^6\text{Li}) - \Delta - 90^\circ_X(^{15}\text{N}) - t_1/2 - 180^\circ_X(^6\text{Li}) - t_1/2 - 90^\circ_\phi(^{15}\text{N}) - t_2(^6\text{Li})$ as described previously.[18] The ^{2}H lock coil of a modified 10-mm broad-band probehead tuned to the frequency of ^{6}Li (44.17 MHz) served as the ^{6}Li observe channel. The broad-band channel of the probe was used to deliver pulses at the frequency

Table IV. Heats of Formation[a] and Selected Geometric Parameters[b] for Lithium Amide Open Dimers and Triple Ions
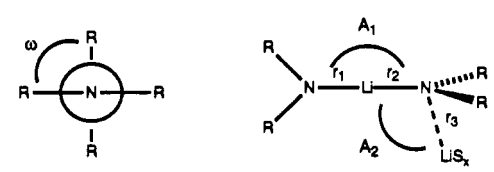
	Hf^a	$r_1{}^b$	r_2	r_3	$r_4{}^c$	A_1	A_2	ω
open dimers								
LiHMDS/2THF	−399.3	1.98	2.25	2.08	2.32	175.7	132.0	68.3
LiHMDS/2HMPA	−355.0	1.99	2.24	2.18	2.24	175.9	140.9	66.4
triple ions								
LiHMDS/4THF	−496.6	2.00	2.00	8.15	2.18	172.9	78.5	87.5
LiHMDS/4HMPA	−411.1	2.00	2.00	9.89	2.18	175.3	105.8	81.1

[a] Enthalpies are listed on a per lithium basis (kcal/mol per Li). [b] Bond distances and angles are measured in angstroms (Å) and degrees, respectively. [c] r_4 corresponds to the average O–Li distance (Å) within the lithium coordination sphere.

Scheme IV
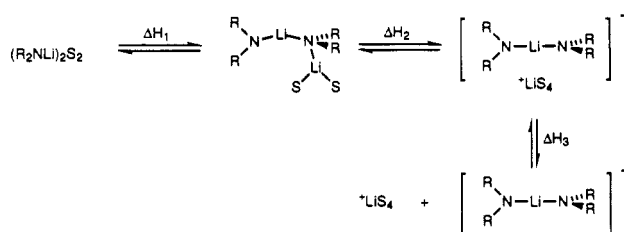
Table V. Heats of Cleavage and Ionization of Cyclic Dimers To Give Open Dimers and Triple Ions (Scheme IV)[a,b]

R₂NLi/S	ΔH_1	ΔH_2	ΔH_3
LiHMDS/THF	−0.2	10.6	36.5
Me₂NLi/THF	8.1	21.2	38.6
LDA/THF	0.5	14.5	35.8
LiTMP/THF	−2.5	10.6	36.0
LiHMDS/HMPA	−2.9	6.2	15.2
Me₂NLi/HMPA	5.4	12.2	17.8
LDA/HMPA	−1.1	9.5	15.5
LiTMP/HMPA	−5.5[c]	5.2[c]	16.7

[a] Enthalpies are listed on a per lithium basis (kcal/mol/Li). [b] The heats of formation of the free ions are as follows: ⁺Li(THF)₄, −135.0; ⁺Li(HMPA)₄, −91.8; [Me₂NLiNMe₂]⁻, −60.5; [*i*-Pr₂NLiN*i*-Pr₂]⁻, −89.2; [TMP-Li-TMP]⁻, −79.0; [(TMS)₂N-Li-N(TMS)₂]⁻, −289.3.

of ¹⁵N (30.42 MHz). Broad-band ¹H decoupling was used at all times during the experiment.[40]

The ³¹P–⁶Li HMQC spectra were recorded in analogy to the ⁶Li–¹⁵N experiments. The sequence was as follows: $90_x^\circ(^{31}P) - \Delta - 90_x^\circ(^6Li) - t_1/2 - 180_x^\circ(^{31}P) - t_1/2 - 90_\phi^\circ(^6Li) - t_2(^{31}P)$. Broad-band ¹H decoupling was used during all periods of the experiment. This affords shift correlation spectra with ³¹P chemical shifts and ³¹P–⁶Li couplings in the f_2 frequency dimension and ⁶Li chemical shifts in the f_1 dimension. The broad-band channel and the ²H lock coil of a modified 10-mm broad-band probehead were used to deliver pulses at the frequencies of ³¹P (121.5 MHz) and ⁶Li, respectively. Pulsing, phase shifting, and detection at the frequency of ³¹P were performed using the multinuclear facilities of the spectrometer. The 90° ³¹P pulse widths were typically 45 μs. Pulses at the frequency of ⁶Li were generated by a BSV-3 BX heteronuclear decoupler with a PTS-160 frequency synthesizer. The 90° ⁶Li decoupler pulse widths were typically 175 μs.

In ⁶Li–¹⁵N and ³¹P–⁶Li HMQC experiments, the preparation delay, Δ, was optimized for the least sensitive triplet in the spectrum of the directly observed nucleus (⁶Li and ³¹P, respectively). Thus $\Delta = {}^1/_4 J_{X-X'}$, where $J_{X-X'}$ is the ⁶Li–¹⁵N or ³¹P–⁶Li coupling constant.[20,41] Both types of HMQC spectra were processed in magnitude mode with squared sine bell weighting in f_1 and Lorentz–Gaussian resolution enhancement in f_2.

The ⁶Li-detected ¹⁵N homonuclear zero-quantum spectra were recorded using the same spectrometer configuration as for the ⁶Li–¹⁵N HMQC experiments. The pulse sequence was as follows:[17,19] $90_x^\circ(^6Li) - \Delta - 180_x^\circ(^6Li)180_x^\circ(^{15}N) - 90_x^\circ(^6Li)90_x^\circ(^{15}N) - t_1 - 90_x^\circ(^6Li)90_\phi^\circ(^{15}N) - t_2(^6Li)$. Broad-band ¹H decoupling was used during all periods of the experiment.[10] Data were processed in phase-sensitive mode with exponential line broadening in f_1 and Lorentz–Gaussian resolution enhancement in f_2.

MNDO Calculations. MNDO calculations were performed on an IBM 3090 supercomputer using MOPAC[21] with lithium parameters of Clark and Theil.[22] All structures were fully optimized under the more rigorous criteria of the keyword PRECISE with no constraints. Each reported heat of formation is the result of a search for the global minimum starting from several different initial geometries. Symmetrical structures were optimized from distorted geometries to insure that the symmetry is not a calculational artifact. For more sterically crowded systems, the keyword GEO-OK was used with caution to override the small interatomic distance check.

Supplementary Material Available: ⁶Li NMR spectra of 0.13 M [⁶Li]LiHMDS and 0.13 M [⁶Li,¹⁵N]LiHMDS, both with added HMPA; ³¹P NMR spectra of 0.13 M [⁶Li]LiHMDS with added HMPA (4 pages). Ordering information is given on any current masthead page.